THE BALTIC JOURNAL
OF ROAD AND BRIDGE ENGINEERING
2026/21(2)

ISSN 1822-427X/eISSN 1822-4288
2026 Volume 21 Issue 2: 31–60
https://doi.org/10.7250/bjrbe.2026-21.677

ASSESSING THE IMPACT OF VEHICLE HETEROGENEITY ON TRAFFIC FLOW EFFICIENCY ON A BRIDGE USING WEIGH-IN-MOTION DATA

JEAN CLAUDE SUGIRA[1], MARC NSHIMIYIMANA[3,4], JEAN DE DIEU NINTERETSE[*,2], PHILEMON NIYOGAKIZA[2]

[1] *School of Transportation Engineering of Southeast University, Nanjing, China*

[2] *School of Civil Engineering of Southeast University, Nanjing, China*

[3] *State Key Laboratory of Geomechanics and Geotechnical Engineering Safety, Institute of Rock and Soil Mechanics, Chinese Academy of Sciences, Wuhan, China*

[4] *University of Chinese Academy of Sciences, Beijing, China*

Received 1 November 2025; accepted 21 May 2026

Abstract. This study investigates how traffic heterogeneity affects both traffic-flow efficiency and bridge structural demand using one year of road-based Weigh-in-Motion (WIM) data collected on a 60 m two-span simply supported prestressed-concrete girder bridge in Nanjing, China. The objective was to develop an integrated framework for quantifying the joint influence of vehicle composition on traffic performance and bridge load effects, and to evaluate whether operational mitigation measures can improve both mobility and structural performance. The methodology combined data preprocessing, vehicle classification, macroscopic traffic-flow modelling, statistical analysis, influence-line-based

* Corresponding author. E-mail: nijeandoss5@gmail.com

Jean Claude SUGIRA (ORCID ID 0009-0007-8383-7509)
Marc NSHIMIYIMANA (ORCID ID 0009-0000-8406-4412)
Jean de Dieu NINTERETSE (ORCID ID 0009-0008-9930-6849)
Philemon NIYOGAKIZA (ORCID ID 0009-0009-4557-9013)

Copyright © 2026 The Author(s). Published by RTU Press

This is an Open Access article distributed under the terms of the Creative Commons Attribution License (http://creativecommons.org/licenses/by/4.0/), which permits unrestricted use, distribution, and reproduction in any medium, provided the original author and source are credited.

structural load-effect estimation, machine-learning prediction, and simulation-based intervention evaluation. Traffic-flow relationships were analysed using the Greenshields's, Greenberg's, and Underwood's models, while XGBoost and SHAP were applied to predict and interpret traffic and structural indicators derived from the processed WIM dataset. The results showed that increasing heavy-vehicle proportion reduced traffic efficiency by lowering flow and speed and increasing density, while simultaneously increasing predicted bending moment, shear force, and fatigue-related demand. Among the calibrated traffic-flow models, the Underwood's model achieved the lowest *RMSE*, while the Greenshields's model remained highly competitive and was retained because of its simpler and more interpretable formulation. The scenario analysis further indicated that both lane management and speed harmonization reduced structural demand relative to the baseline observed traffic condition, with lane management providing the greater overall benefit. The proposed framework is intended as an analytical and scenario-based decision-support methodology for evaluating bridge traffic-management strategies under heterogeneous traffic conditions.

Keywords: computer simulations, macroscopic traffic models, machine learning, traffic flow, traffic simulation, vehicle heterogeneity, Weigh-in-Motion.

Introduction

Bridges are critical links in highway networks, but they are also traffic environments in which operational efficiency is especially sensitive to vehicle heterogeneity. Compared with ordinary freeway segments, bridge sections often have narrow usable cross-sections, limited shoulders, constrained lane-changing opportunities, and more concentrated lane utilisation near approaches and exits. Under these conditions, the interaction between passenger cars and heavy vehicles becomes more pronounced, particularly when traffic demand approaches capacity (Sugira et al., 2023). Empirical studies have shown that increasing truck proportions can reduce speed, alter headway patterns, and lower traffic throughput. For example, Roh et al. (2017) reported a clear decrease in operating speeds on multilane freeway sections as truck share increased, while Saifuzzaman & Zheng (2014) showed that heavy vehicles generally maintain longer headways, travel more slowly, and require more time to merge than passenger cars. These effects are especially important on bridge segments, where geometric and operational constraints amplify the influence of heterogeneous traffic. Vehicle heterogeneity on bridges is not only a traffic-flow issue; it is also a structural loading issue. Heavy vehicles contribute disproportionately to axle-load effects, peak bending moments, shear forces, and cumulative fatigue demand. Using site-specific WIM data, Nowak & Szerszen (2000) showed that truck-induced fatigue stress spectra in bridge girders could exceed simplified code expectations, while Gokce et al. (2011) demonstrated that deterministic bridge rating approaches might underestimate bending and shear demand under realistic traffic loading. In other words, the same traffic composition that degrades flow efficiency can also intensify structural demand.

For freight-intensive corridors, this dual role of heavy vehicles means that bridge traffic management ideally considers both mobility performance and infrastructure preservation rather than treating them as unrelated objectives.

Recent advances in monitoring technologies provide an opportunity to study these two dimensions using measured vehicle data. At a basic level, it is important to distinguish between road-based Weigh-in-Motion (WIM) systems and Bridge Weigh-in-Motion (B-WIM) systems. Road-based WIM systems are installed in or on the pavement and estimate vehicle characteristics such as gross vehicle weight, axle loads, axle spacing, speed, and classification while vehicles pass over the instrumented section. By contrast, B-WIM systems use the bridge itself as the weighing scale and infer vehicle loads from measured bridge responses, typically strain-based or other structural-response measurements (Sujon & Dai, 2021; Žnidarič & Kalin, 2020). This distinction is essential because the sensing principle, calibration procedure, and interpretation of the measured data differ substantially between the two approaches. Within the B-WIM literature, technology can be viewed from at least two complementary perspectives. The first concerns vehicle detection and axle identification (Cartiaux et al., 2023). Earlier systems relied on conventional axle detectors or contact-type devices, whereas more recent approaches use free-of-axle-detector/nothing-on-the-road concepts in which sensors installed under the bridge identify axle passages without intrusive pavement instrumentation (Dong et al., 2023). Wavelet-based strain processing has been used to improve axle detection in such systems, and it has also demonstrated virtual axle detection using bridge acceleration measurements and convolutional neural networks (Zhao et al., 2024). The second perspective concerns the identification of axle-load and gross weight. The classical B-WIM framework follows the Moses influence-line concept, while later developments extended the field toward dynamic and inverse-problem formulations such as moving force identification; more recent studies have also explored contactless vision-assisted and machine-learning-supported identification strategies (González et al., 2008). Introducing these distinctions is necessary to avoid conceptual ambiguity when discussing measured traffic data, bridge response, and subsequent prediction models.

At the same time, machine-learning methods are increasingly being used to capture nonlinear relationships in transportation data. Gradient-boosting methods such as XGBoost have shown strong predictive performance for structured tabular datasets because they can model complex interactions among traffic composition, density, speed, temporal factors, and vehicle attributes (Chen & Guestrin, 2016). SHAP provides a theoretically grounded framework for interpreting such models by quantifying the contribution of each feature to the prediction outcome (Lundberg & Lee, 2017). However, in the present study, machine learning is not treated as a substitute for the monitoring system itself. Instead, the monitoring data provides the empirical description of the traffic stream, from which traffic and structural indicators are derived, while the machine-learning model is used in a subsequent step to predict these indicators and interpret the relative importance of heterogeneity-related variables. Clarifying this sequence is important because the physical measurement system and the predictive model serve different roles within the overall analytical framework (Ruiz et al., 2025). Accordingly, the research gap addressed in this study is not that traffic analysis and bridge-response analysis are universally independent in literature. In fact, B-WIM research has long relied on the direct relationship between vehicle loads and bridge response, and B-WIM measurements have also been used to derive bridge performance indicators and support structural monitoring. The gap addressed here is more specific: although measured vehicle data are increasingly available, relatively few studies use a single monitored traffic dataset to jointly quantify the effect of vehicle heterogeneity on both traffic-flow efficiency and bridge load effects and then extend that joint assessment to the evaluation of practical traffic-management strategies. Existing studies often emphasise either operational traffic performance or structural demand, whereas the translation of measured heterogeneity into operational decisions that can benefit both objectives remains limited.

To address this gap, this study develops an integrated analytical framework using one year of WIM-based vehicle data collected at a highway bridge site in China. First, the study quantifies how increasing heavy-vehicle proportion affects key traffic variables, including flow, density, and speed, through calibrated macroscopic traffic-flow models. Second, the same monitored traffic stream is used to estimate bridge-related response indicators, including bending moment, shear force, and fatigue-related demand. Third, XGBoost combined with SHAP is applied to predict and interpret the influence of heterogeneity-related features on both traffic and structural indicators. Finally, the resulting relationships are incorporated into a simulation-based evaluation of mitigation measures, including dedicated truck-lane organisation and speed harmonization, to examine whether such interventions can improve traffic performance while reducing adverse structural demand.

The contribution of this study is therefore threefold. First, it provides a joint assessment of the operational and structural consequences of traffic heterogeneity on a bridge segment using a common monitored dataset. Second, it combines physically interpretable traffic-flow and load-effect analysis with explainable machine-learning prediction. Third, it extends the analysis toward decision support by evaluating intervention scenarios that target both traffic efficiency and bridge preservation. In this way, the study aims to support more balanced bridge traffic management strategies for freight-intensive corridors, where maintaining throughput and protecting infrastructure should be considered simultaneously rather than separately. The proposed framework is a decision-support workflow, not a deployed real-time control system. It uses road-WIM data to quantify the joint effect of vehicle heterogeneity on traffic-flow efficiency and bridge load effects and then evaluates candidate mitigation strategies through predictive modelling and microsimulation. The framework, therefore supports operational assessment and scenario testing rather than autonomous control.

1. Methodology

This study adopted an integrated methodology to evaluate how traffic heterogeneity affects both traffic-flow efficiency and bridge structural demand using one year of road-WIM data. The workflow consisted of: (i) defining the overall analytical framework, (ii) describing the study site, bridge, and monitoring system, (iii) preprocessing and classifying the WIM data, (iv) deriving interval-based traffic variables, (v) calibrating macroscopic traffic-flow models, (vi) estimating structural load effects, (vii) applying machine-learning models for prediction and interpretation, and (viii) evaluating mitigation scenarios through simulation. This structure was used to ensure that each step of the analysis could be clearly linked to the corresponding results presented later in the manuscript.

1.1. Overall framework and decision logic

Figure 1 illustrates the overall framework adopted in this study. The proposed approach is a decision-support workflow based on road-WIM data, rather than a deployed real-time control system. Its purpose is to quantify how traffic heterogeneity affects both traffic-flow efficiency and bridge load effects, and then to evaluate candidate mitigation strategies.

First, vehicle-level road-WIM records, including speed, axle count, axle spacing, axle loads, gross vehicle weight, and lane information, are collected and preprocessed. Invalid observations are removed, and vehicles are classified into passenger cars, light trucks, and heavy trucks. The cleaned data are then aggregated to derive key traffic variables such as flow, speed, density, and heavy-vehicle proportion.

Second, the same monitored traffic stream is used to estimate structural load effects at the critical bridge sections, including maximum bending moment, maximum shear force, and fatigue-related demand. In parallel, XGBoost and SHAP are applied to predict and interpret the influence of traffic heterogeneity on both operational and structural indicators.

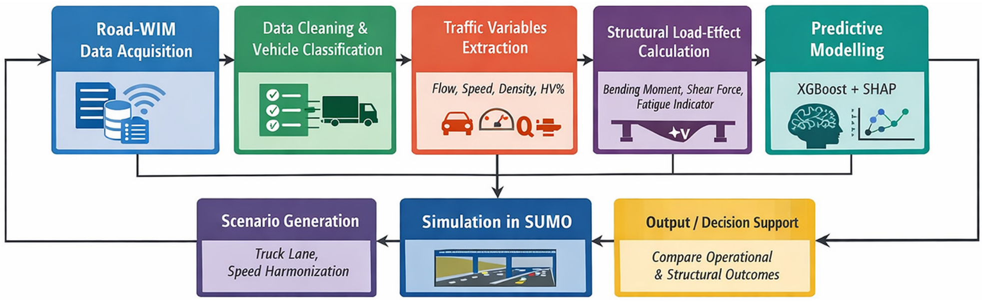

Figure 1. Overall decision-support framework of the study

Finally, candidate mitigation strategies, including dedicated truck-lane organization and speed harmonization, are tested in SUMO (Lopez et al., 2018). Their effectiveness is evaluated by jointly comparing traffic performance and structural response. Therefore, the framework serves as an integrated methodology for supporting bridge traffic-management decisions under heterogeneous traffic conditions.

1.2. Study site and bridge characteristics

The study used one year of traffic records collected from 1 January to 31 December 2023 on a two-span simply supported highway bridge located in Nanjing City, China. The bridge carries two lanes of opposite-direction traffic, with one lane per direction and a lane width of 3.0 m. The longitudinal geometry consists of two simply supported spans of 30 m each, giving a total bridge length of 60 m. Structurally, the bridge is a prestressed-concrete girder bridge with a deck slab superstructure and was in normal service condition during the monitoring period. The cross-sectional arrangement therefore comprises a deck slab supported by prestressed-concrete girders serving the two traffic lanes. These characteristics define the structural context in which the monitored traffic stream was analysed.

In the present study, the structural effects were evaluated on the deck slab of the critical span. The reported maximum bending moment corresponds to the maximum instantaneous bending moment at midspan, while the reported maximum shear force corresponds to the maximum instantaneous shear force at the support section of the same span. These bridge characteristics are reported to ensure that the traffic-flow analysis, structural load-effect estimation, and fatigue-related results are interpreted within a clear and reproducible structural framework.

1.3. Road-based WIM system and data acquisition

The monitoring system used in this study was a road-based Weigh-in-Motion (WIM) installation rather than a Bridge Weigh-in-Motion (B-WIM) system. This distinction is important because road-based WIM systems estimate vehicle characteristics using pavement-installed sensors, whereas B-WIM systems infer vehicle loads from the measured structural response of the bridge itself (Adresi et al., 2024). In the present study, the monitored data were therefore obtained from roadway instrumentation and subsequently used as input for both traffic and structural analyses.

The road-WIM station was equipped with quartz piezoelectric sensors installed in the carriageway (Adresi et al., 2024). For each passing vehicle, the system recorded the time of passage, lane, speed, number of axles, axle spacing, individual axle loads, and gross vehicle weight. These vehicle-level outputs formed the basis for the subsequent traffic-flow analysis, structural load-effect estimation, machine-learning prediction, and simulation-based evaluation conducted in this study. The available dataset consisted of processed WIM records collected continuously from 1 January to 31 December 2023 at the monitored bridge site in Nanjing, China. Since the system operated as an in-service calibrated road-WIM station, all recorded vehicle observations were subjected to further quality-control filtering before analysis. Records with missing or physically implausible values, including unrealistic speeds, gross vehicle weights, axle loads, axle counts, and time stamps, were removed during preprocessing to ensure consistency and reliability of the final dataset.

To improve transparency, the road-WIM system should be interpreted in this study as the primary traffic-data source, while the bridge structural effects were estimated analytically from the measured axle streams rather than being measured directly from bridge-response sensors. This distinction is essential for correctly understanding the scope of the proposed framework and the methodological relationship between monitored traffic data and the derived bridge load effects.

1.4. Data preprocessing and vehicle classification

Raw road-WIM records were screened before analysis to remove incomplete and physically implausible observations. A vehicle record was excluded if it contained invalid lane or time information, missing axle-related measurements, speeds below 5 km/h or above 120 km/h, non-positive axle loads, or gross vehicle weights exceeding 100 t. Duplicate and inconsistent records were also removed. These filtering steps ensured that only reliable vehicle-level observations were retained for further analysis. After quality control, the cleaned dataset was classified into three operational vehicle groups according to gross vehicle weight. The adopted classification scheme was:

C1: Passenger cars if $GVW < 3.5$ t,
C2: Light trucks if $3.5 \le GVW < 20$ t,
C3: Heavy trucks if $GVW \ge 20$ t.

In this classification, axle count was used as a descriptive characteristic rather than a strict exclusion rule. The corresponding class definitions and representative vehicle types are summarised in Table 1, while the resulting class distribution in the cleaned road-WIM dataset is reported in Table 2.

To support the subsequent traffic-flow analysis, the cleaned vehicle-level records were aggregated into 15-minute intervals. For each interval m, traffic flow q_{m} was computed as

$$q_{\mathrm{m}} = \frac{N_{\mathrm{m}}}{\Delta t}, \tag{1}$$

where N_{m} is the number of vehicles observed in interval and $\Delta t = 0.25$ h. The mean speed was calculated as

$$\bar{v}_{\mathrm{m}} = \frac{1}{N_{\mathrm{m}}} \sum_{i=1}^{N_{\mathrm{m}}} v_i, \tag{2}$$

where v_i is the speed of vehicle i. Traffic density k_{m} was then estimated from

$$k_{\mathrm{m}} = \frac{q_{\mathrm{m}}}{\bar{v}_{\mathrm{m}}}. \tag{3}$$

The heavy-vehicle proportion in interval m was defined as

$$HV_{\mathrm{m}} = \frac{N_{\mathrm{C3,m}}}{N_{\mathrm{m}}} \times 100\% \tag{4}$$

where $N_{\mathrm{C3,m}}$ is the number of heavy trucks in that interval. These interval-based variables formed the basis for the macroscopic traffic-flow modelling, statistical analysis, machine-learning prediction, and simulation-based scenario evaluation presented in the following sections.

Table 1. Vehicle classification scheme adopted in the study

Class	Operational category	*GVW*	Typical axle count	Representative vehicle type
C1	Passenger cars	*GVW* < 3.5 t	2	Sedan, hatchback, SUV, pickup
C2	Light trucks	3.5 ≤ *GVW* < 20 t	2–3	Light commercial truck, small delivery truck, minibus / small bus
C3	Heavy trucks	*GVW* ≥ 20 t	≥ 3	Multi-axle rigid truck, tractor-semitrailer, articulated freight truck

1.5. Macroscopic traffic-flow modelling and statistical analysis

To characterise the effect of traffic heterogeneity on bridge traffic operations, three classical macroscopic traffic-flow models were calibrated: Greenshields (Wang et al., 2011), Greenberg (Greenberg, 1959), and Underwood (Kockelman, 2001). The Greenshields's model assumes a linear speed-density relationship:

$$v = v_{\mathrm{f}}\left(1\frac{k}{k_{\mathrm{j}}}\right), \tag{5}$$

where v_{f} is free-flow speed and k_{j} is jam density. The associated flow is

$$= kv = kv_{\mathrm{f}}\left(1\frac{k}{k_{\mathrm{j}}}\right). \tag{6}$$

The Greenberg's model is given by

$$v = v_{\mathrm{m}}\ln\left(\frac{k_{\mathrm{j}}}{k}\right) \tag{7}$$

with the corresponding flow

$$= kv_{\mathrm{m}}\ln\left(\frac{k_{\mathrm{j}}}{k}\right). \tag{8}$$

The Underwood's model assumes

$$v = v_{\mathrm{f}}\exp\left(-\frac{k}{k_0}\right), \tag{9}$$

and the corresponding flow is

$$q = kv_{\mathrm{f}}\exp\left(-\frac{k}{k_0}\right). \tag{10}$$

All three models were calibrated using the 15-minute interval data derived from the clean road-WIM records. To examine the effect of traffic heterogeneity, the calibration was carried out separately for different heavy-vehicle proportion groups. The fitted models were then compared using their goodness of fit and error statistics, and the best-performing model was selected for subsequent interpretation of traffic behaviour on the bridge. To examine statistical differences among heavy-vehicle composition groups, one-way ANOVA was applied. The ANOVA statistic was computed as

$$F = \frac{SS_{\mathrm{B}}/(g-1)}{SS_{\mathrm{W}}/(N-g)}, \tag{11}$$

where SS_B and SS_W are the between-group and within-group sums of squares, respectively, g is the number of groups, and N is the total number of observations. The monotonic association between heavy-vehicle proportion and traffic/structural indicators was quantified using Spearman's rank correlation coefficient:

$$\rho_\mathrm{s} = 1 - \frac{6\sum_{i=1}^{n} d_i^2}{n\left(n^2 - 1\right)}, \tag{12}$$

where d_i is the difference between paired ranks.

1.6. Structural load-effect estimation

Structural load effects were estimated from the measured axle streams using an influence-line-based moving-load model. For each vehicle, the road-WIM record provided axle loads, axle spacings, lane, speed, and entry time. These inputs were used to reconstruct the longitudinal position of each axle at successive time steps as the vehicle crossed the bridge. When multiple vehicles were present on the bridge simultaneously, their load effects were superposed to account for multiple-presence events. In this study, the structural responses were evaluated on the deck slab of the critical span. Accordingly, the bending moment time history was computed as

$$M_\mathrm{s}\left(t\right) = \sum_i \sum_j P_{ij}\, I_\mathrm{M}\left(x_{ij}\left(t\right), s\right), \tag{13}$$

where P_{ij} is the load of axle j of vehicle i, $x_{ij}(t)$ is the axle position at time t, and I_M is the bending-moment influence ordinate at the selected section s. Similarly, the shear force time history was obtained as

$$V_\mathrm{s}\left(t\right) = \sum_i \sum_j P_{ij}\, I_\mathrm{V}\left(x_{ij}\left(t\right), s\right), \tag{14}$$

where I_V is the corresponding shear influence ordinate at section s. The maximum structural effects reported in the Results section were extracted from these time histories as

$$M_\mathrm{s,max} = \max_t M_\mathrm{s}\left(t\right), V_\mathrm{s,max} = \max_t V_\mathrm{s}\left(t\right). \tag{15}$$

Fatigue-related demand was evaluated using Palmgren-Miner linear damage accumulation (Blacha, 2021). The stress-range history derived from the simulated load-effect history was converted into fatigue cycles, and the cumulative fatigue damage index was calculated as

$$D = \sum_r \frac{n_r}{N_r}, \tag{16}$$

where n_r is the number of observed stress cycles in range r, and N_r is the corresponding fatigue life obtained from the adopted fatigue relationship. In this way, the fatigue indicator was used to compare the relative cumulative structural demand under different traffic compositions and mitigation scenarios. Thus, the structural load-effect analysis in this study was based on road-WIM-informed analytical estimation, not direct bridge-response sensing. The resulting bending moment, shear force, and fatigue indicators therefore represent analytically derived structural-demand measures driven by the measured traffic stream.

1.7. Machine-learning models, validation, and simulation-based intervention assessment

Machine learning was used in this study as a supervised regression tool to predict traffic and structural indicators from the processed road-WIM dataset. The purpose of this stage was not to replace the physical traffic-flow or structural load-effect calculations, but to develop predictive surrogate models capable of capturing the relationship between traffic heterogeneity, vehicle-loading characteristics, and the resulting operational and structural indicators. The input features were derived from the cleaned road-WIM records and the aggregated traffic dataset and included heavy-vehicle proportion, traffic density, mean speed, gross vehicle weight, average axle load, inter-vehicle spacing, hour of day, and day of week. Separate target variables were defined for traffic flow, maximum bending moment, and maximum shear force. Two ensemble learning algorithms were tested: Random Forest (RF) and Extreme Gradient Boosting (XGBoost). Random Forest was used as a benchmark model for nonlinear regression, while XGBoost was selected as the main predictive model because of its strong performance for structured tabular datasets and its ability to capture complex nonlinear interactions among traffic and vehicle-related variables. The dataset was divided into a training subset (80%) and an independent test subset (20%). Hyperparameter tuning was carried out using ten-fold cross-validation within the training set to reduce overfitting and improve generalization. Final performance was evaluated on the held-out test set using the coefficient of determination (R^2), root mean square error ($RMSE$), and mean absolute error (MAE), all reported in the original physical units of the target variables. Accordingly, the machine-learning validation reflects the ability of the models to reproduce the WIM-informed analytical outputs used in this study, rather than direct validation against independently measured bridge-response signals. For the macroscopic traffic-flow models, validation was based on the agreement between the observed and model-predicted speed-density-flow relationships derived from the processed road-WIM dataset. The performance of the Greenshields's, Greenberg's, and Underwood's models was compared across the heavy-vehicle proportion groups defined in the preprocessing stage in order to identify the most suitable representation of heterogeneous bridge traffic conditions. To improve interpretability of the machine-learning stage, SHAP (SHapley Additive exPlanations) was applied to the final XGBoost models to quantify the contribution of each input feature to the predicted target variables and to identify the dominant explanatory factors governing traffic-flow performance and structural load effects.

The final stage of the framework involved microscopic simulation-based intervention assessment using SUMO. The simulation model was calibrated using the observed traffic composition, heavy-vehicle operating characteristics, and lane-changing behaviour derived from the monitored site. In the calibrated setup, the heavy-vehicle acceleration parameter was set to 0.8 m/s^2, and lane changing was restricted within 50 m of the bridge ends. The agreement between simulated and observed traffic flow was assessed using the GEH statistic. Two non-restrictive intervention scenarios were then evaluated: lane management and speed harmonization with a 70 km/h control speed. For each scenario, the simulated trajectories were converted into updated traffic variables and then re-evaluated using the same structural load-effect model to estimate the resulting changes in flow, density, maximum bending moment, maximum shear force, and fatigue-related demand. In this way, the machine-learning and simulation components acted as predictive and evaluative layers within the overall framework, supporting both interpretation and scenario-based decision making.

2. Numerical study

2.1. Characteristics of road-WIM data and vehicle classification

The traffic data analysed in this study were collected using a road-based WIM system installed at a 60 m two-span simply supported bridge in Nanjing, China. The bridge carries two lanes of opposite-direction traffic, with one lane per direction and a lane width of 3.0 m. The monitoring period covered one full year, from 1 January to 31 December 2023. Following the preprocessing procedure described in Section 2.3, records with invalid lane or time information, missing axle-related measurements, speeds below 5 km/h or above 120 km/h, non-positive axle loads, and gross vehicle weights exceeding 100 t were excluded. After quality control, the final cleaned dataset contained 8 041 800 vehicle records, which formed the basis for all subsequent traffic and structural analyses. For operational analysis, the cleaned vehicle records were classified into three groups according to the scheme defined in Table 1: C1 (passenger cars), C2 (light trucks), and C3 (heavy trucks). The resulting class distribution is summarised in Table 1. Passenger cars (C1) dominated the traffic stream, accounting for 83.22% of all observed vehicles, with a mean gross vehicle weight of 1.39 t and a mean speed of 60.57 km/h. Light trucks (C2) represented 10.52% of the traffic stream, with a mean gross vehicle weight of 10.29 t and a mean speed of 51.21 km/h. Heavy trucks (C3) accounted for 6.26% of the dataset and exhibited the highest mean gross vehicle weight (35.68 t) together with the lowest mean speed (45.73 km/h), as shown in Table 2. These results indicate that although passenger cars dominate the bridge traffic numerically, the freight component remains substantial and is characterized by lower operating speeds and higher axle-related demand. In particular, the heavy-truck class represents the most important source of traffic heterogeneity for both traffic-flow degradation and bridge structural loading.

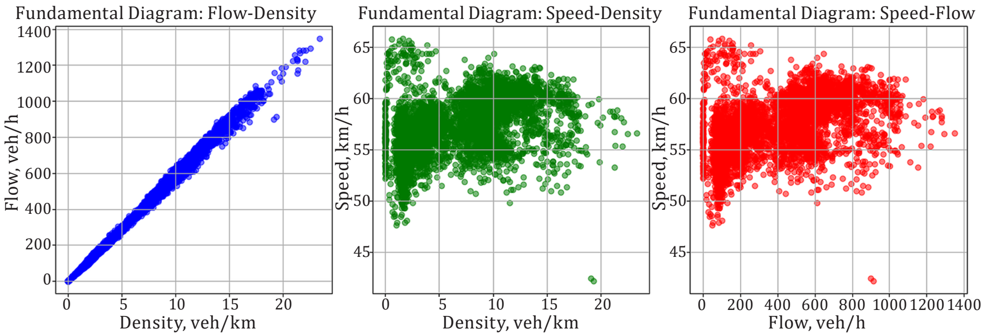

Figure 2. Fundamental relationship among traffic density, flow, and speed derived from the cleaned 15-minute road-WIM dataset

To support the subsequent traffic-flow analysis, the cleaned vehicle-level records were aggregated into 15-minute intervals, from which flow, speed, density, and heavy-vehicle proportion were derived. The resulting macroscopic relationships are shown in Figure 2, while the influence of heavy-vehicle proportion and daily traffic periods is illustrated in Figure 3(a) and Figure 3(b). As shown in Figure 2, the observed flow-density relationship is predominantly increasing over the analysed range, indicating that most of the dataset corresponds to uncongested to near-capacity traffic conditions. A similar trend is observed in Figure 3(b), where both peak and non-peak observations show increasing flow with increasing density, although the peak-hour condition is associated with higher densities and higher flows overall. Therefore, the present dataset does not clearly exhibit a fully developed congested branch in which higher density corresponds to lower flow. For this reason, higher density should not be interpreted here as being generally associated with lower flow. By contrast, Figure 3(a) shows a clearer and more consistent relationship between heavy-vehicle proportion and traffic flow. In general, higher heavy-vehicle shares are associated with lower traffic flow, particularly during non-peak conditions, indicating the adverse influence of heavy vehicles on traffic efficiency. The marker sizes in Figure 3(a) represent traffic density and show that a wide range of density values is present across the observations; however, the dominant pattern in this figure is the negative association between heavy-vehicle proportion and flow, rather than a monotonic negative association between density and flow.

Thus, results of this section confirm that the cleaned road-WIM dataset captures both the dominant contribution of passenger cars and the structurally important influence of heavier freight traffic. The dataset therefore provides a suitable basis for the macroscopic traffic-flow modelling, structural load-effect estimation, and machine-learning analysis presented in the following sections.

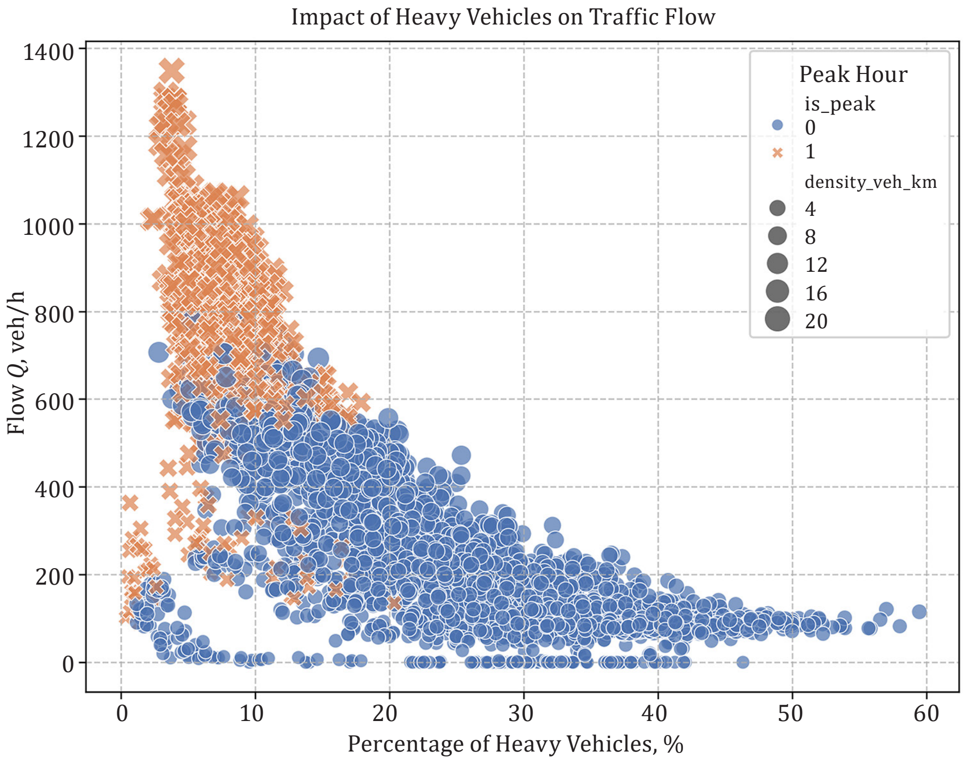

Figure 3(a). Relationship between heavy-vehicle proportion and traffic flow, with marker size representing traffic density

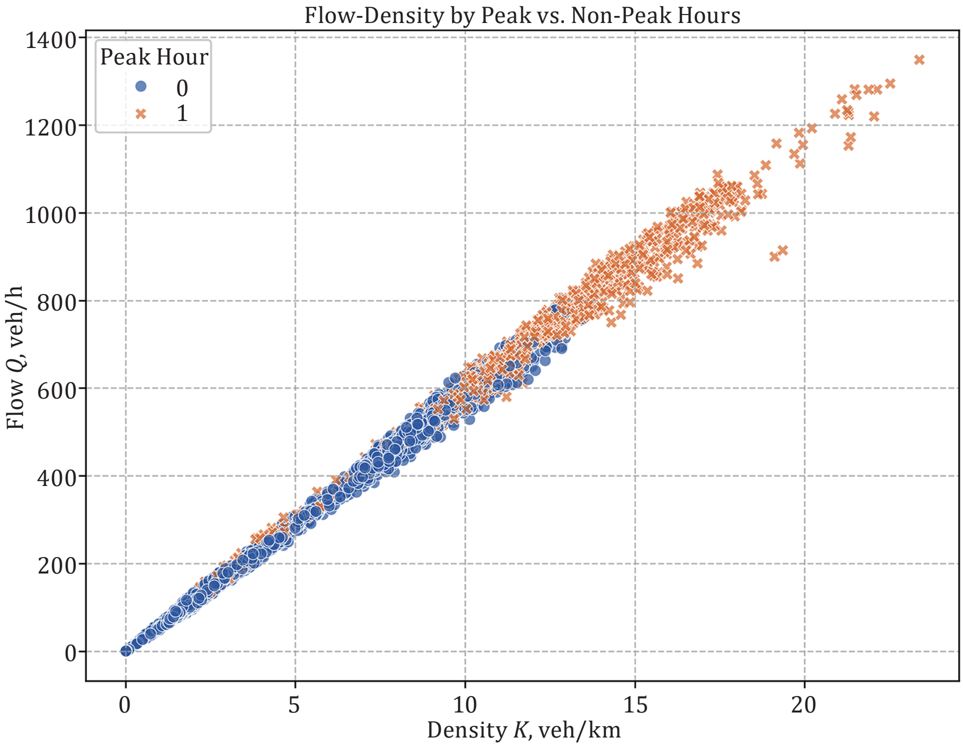

Figure 3(b). Comparison of flow-density characteristics under peak and non-peak traffic conditions

Table 2 summarises the operational vehicle classification in the cleaned road-WIM dataset. Passenger cars (C1) dominated the traffic stream, accounting for 83.22% of all recorded vehicles, with a mean gross vehicle weight of 1.39 t and a mean speed of 60.57 km/h. Light trucks (C2) represented 10.52% of the dataset and showed a mean gross vehicle weight of 10.29 t and a mean speed of 51.21 km/h. Heavy trucks (C3) accounted for 6.26% of the traffic stream, but exhibited the highest mean gross vehicle weight (35.68 t) and the lowest mean speed (45.73 km/h). These results indicate that although passenger cars dominate bridge traffic numerically, heavy trucks contribute disproportionately to the high-load portion of the traffic stream and therefore play a critical role in both traffic heterogeneity and bridge structural demand.

Table 2. Operational vehicle classification results obtained from the cleaned road-WIM dataset

Class	Operational category	Observed modal axle count	Proportion, %	Vehicle count	Mean *GVW*, t	Mean speed, km/h	Mean number of axles
C1	Passenger cars	2	83.22	6 692 704	1.39	60.57	2.05
C2	Light trucks	2	10.52	845 864	10.29	51.21	3.19
C3	Heavy trucks	6	6.26	503 232	35.68	45.73	4.93

The axle-count values reported in Table 2 represent the dominant observed axle configuration within each class in the cleaned road-WIM dataset and are presented for descriptive purposes only. The operational classification itself was defined primarily by gross vehicle weight, with axle count used as a supporting characteristic.

2.2. Macroscopic model calibration

The calibration results of the three macroscopic traffic-flow models are summarised in Table 3, and the corresponding fitting curves are shown in Figure 4. All three models reproduced the general trend of the observed bridge traffic data, although their goodness of fit and error statistics differed slightly. The Greenshields's model achieved an R^2 of 0.996 with an *RMSE* of 19.2 veh/h, while the Underwood's model produced a slightly lower *RMSE* of 19.1 veh/h and an R^2 of 0.991. The Greenberg model showed comparatively weaker performance, with an R^2 of 0.961 and an *RMSE* of 24.8 veh/h.

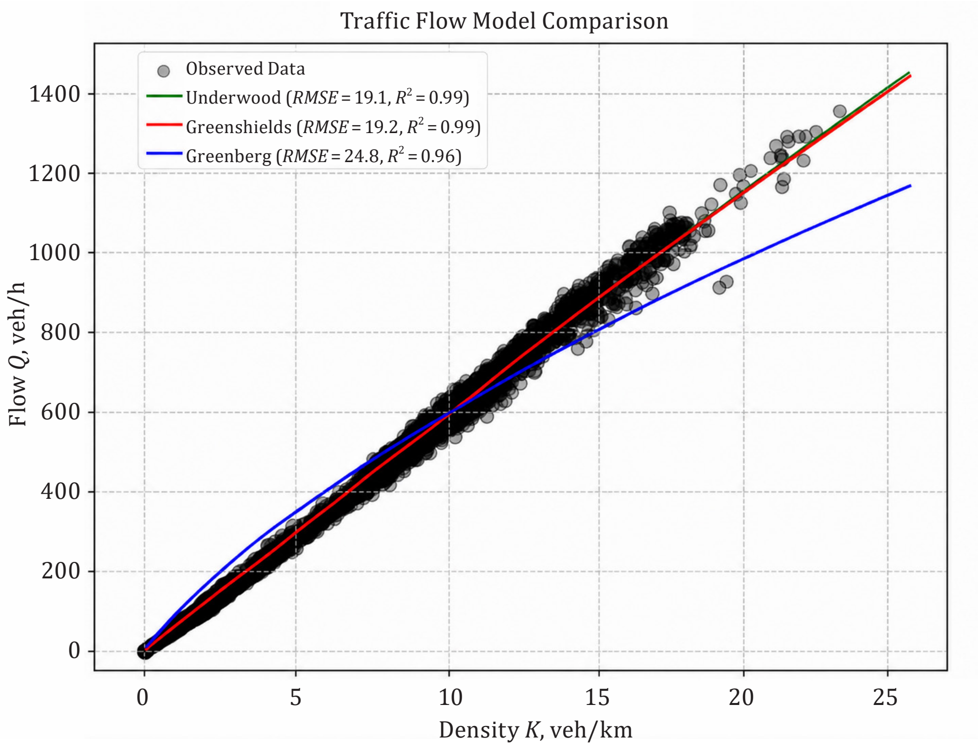

Figure 4. Macroscopic models fitting results and performance

Table 3. Calibration Results for Macroscopic Models

Model	R^2	*RMSE*, veh/h	v_f, km/h	k_j, veh/km/lane
Greenshields	0.996	19.2	80.2	119.8
Greenberg	0.961	24.8	–	120.5
Underwood	0.991	19.1	80.0	–

Although the Underwood's model provided the lowest *RMSE*, the difference relative to the Greenshields's model was very small. The Greenshields's model was therefore retained for subsequent interpretation because it combined strong predictive performance with a simpler and more directly interpretable linear speed-density relationship. Under heterogeneous bridge traffic conditions, where lane confinement and heavy-vehicle presence intensify vehicle interactions, this formulation provided a practical basis for describing the observed traffic behaviour.

The calibrated Greenshields's relationship is expressed as:

$$q = k \times 80.2\left(1 - \frac{k}{119.8}\right), \tag{17}$$

where q is traffic flow (veh/h/lane) and k is density (veh/km/lane). Under free-flow conditions, the calibrated model predicts a maximum flow of 2403 veh/h/lane at an optimal density of 59.9 veh/km/lane. As the proportion of heavy vehicles increased, the estimated traffic capacity declined. For example, at a truck composition of approximately 15%, the maximum flow decreased by 6.7%, while the critical density shifted slightly to 62.5 veh/km/lane. The sensitivity analysis further indicated that each additional 5% increase in truck proportion was associated with an approximate reduction of 135 veh/h/lane in maximum flow, highlighting the adverse influence of heavy vehicles on bridge traffic efficiency.

2.3. Statistical analysis outcomes

Based on the heavy-vehicle proportion groups defined in the preprocessing stage, one-way ANOVA and Spearman correlation were applied to evaluate the influence of traffic heterogeneity on flow, speed, and density. One-way ANOVA results demonstrated that the proportion of heavy vehicles had a statistically significant effect on all key traffic flow parameters. Specifically, flow showed a strong effect size with

$$(3{,}34992) = 124.5,\ p < 0.001 \text{ (flow)},\ \eta 2 = 0.15,$$
$$(3{,}34992) = 112.3,\ p < 0.001 \text{ (speed)},\ \eta 2 = 0.14,$$
$$(3{,}34992) = 98.7,\ p < 0.001 \text{ (density)},\ \eta 2 = 0.12.$$

Post-hoc Tukey HSD [24] Comparisons further indicated a significant decrease in flow by approximately 150 vehicles/h/lane ($p < 0.01$) when heavy truck proportions exceeded 10%. Spearman's rank correlation analysis confirmed strong monotonic relationships between heavy vehicle percentage and traffic characteristics:

$$\rho = -0.81 (p < 0.001, \text{flow vs. \% heavy vehicles}),$$
$$\rho = -0.79 (p < 0.001, \text{speed vs. \% heavy vehicles}),$$
$$\rho = 0.76 (p < 0.001, \text{density vs. \% heavy vehicles}).$$

These correlations indicate a consistent decline in traffic performance as the proportion of heavy vehicles increases.

2.4. Machine-learning performance

To further quantify the relationship between traffic heterogeneity and bridge-related performance indicators, supervised machine-learning models were trained using the processed road-WIM dataset described in Section 2. Separate models were developed for traffic flow, maximum bending moment, and maximum shear force using traffic descriptors, vehicle characteristics, and temporal variables derived from the cleaned dataset. Among the tested algorithms, XGBoost consistently outperformed Random Forest (RF) across all target variables. As shown in Table 4, XGBoost achieved higher values and lower *RMSE* and *MAE* values than RF for flow, bending moment, and shear force prediction. The reported performance metrics were computed on the independent test set and are presented in the original engineering units of the target variables. These results indicate that gradient-boosted tree models were more effective in capturing the nonlinear relationship between traffic heterogeneity, vehicle-loading characteristics, and the resulting traffic and structural indicators.

Table 4. Predictive accuracy of machine-learning models

Target variable	Algorithm	R^2	*RMSE*	*MAE*
Flow, veh/h/lane	XGBoost	0.958	48.6 veh/h	32.4 veh/h
	RF	0.934	67.9 veh/h	45.8 veh/h
Maximum bending moment, kNm	XGBoost	0.947	41.8 kNm	28.7 kNm
	RF	0.921	57.6 kNm	39.5 kNm
Maximum shear force, kN	XGBoost	0.938	24.9 kN	17.6 kN
	RF	0.909	33.8 kN	23.4 kN

2.5. SHAP analysis: Feature-importance interpretation

Figures 5 and 6 present the SHAP-based interpretation of the XGBoost models for traffic-flow and structural-response prediction, respectively. The SHAP results quantify how the explanatory variables contributed to the model outputs and therefore provide insight into the relative influence of traffic heterogeneity on both operational and structural indicators. In both models, the percentage of heavy vehicles emerged as the dominant predictor, confirming its central role in explaining reductions in traffic efficiency and increases in bridge-related load effects. For the traffic-flow model, the SHAP results indicate that increasing heavy-vehicle proportion was associated with lower predicted flow capacity, particularly under higher-density conditions. For the structural-response model, the same increase in heavy-vehicle proportion was associated with larger predicted maximum bending moments. These findings are consistent with the statistical results presented earlier and support the conclusion that traffic heterogeneity affects bridge operation through two coupled mechanisms: deterioration of traffic performance and amplification of structural demand (Sugira et al., 2026).

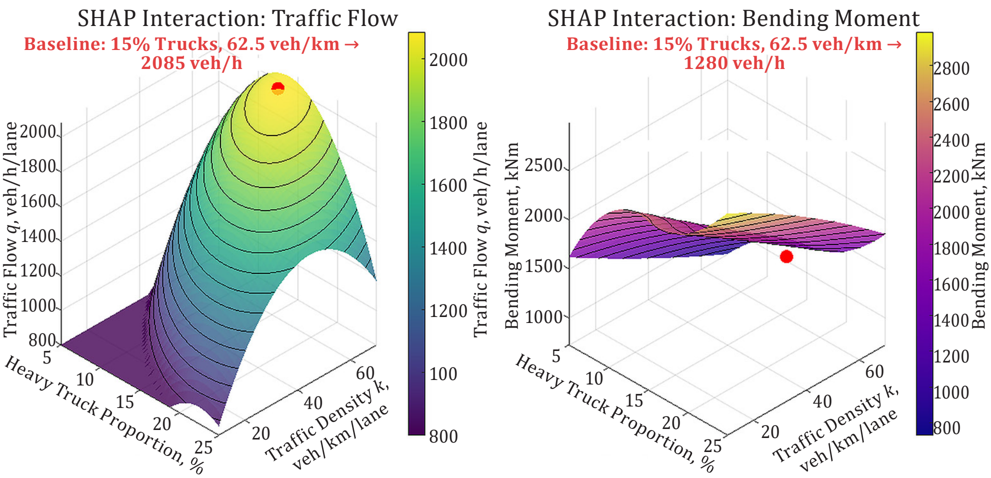

Figure 5. SHAP-based interpretation of the XGBoost traffic-flow model, showing the interaction effects of heavy-vehicle proportion, traffic density, and inter-vehicle spacing on predicted flow performance

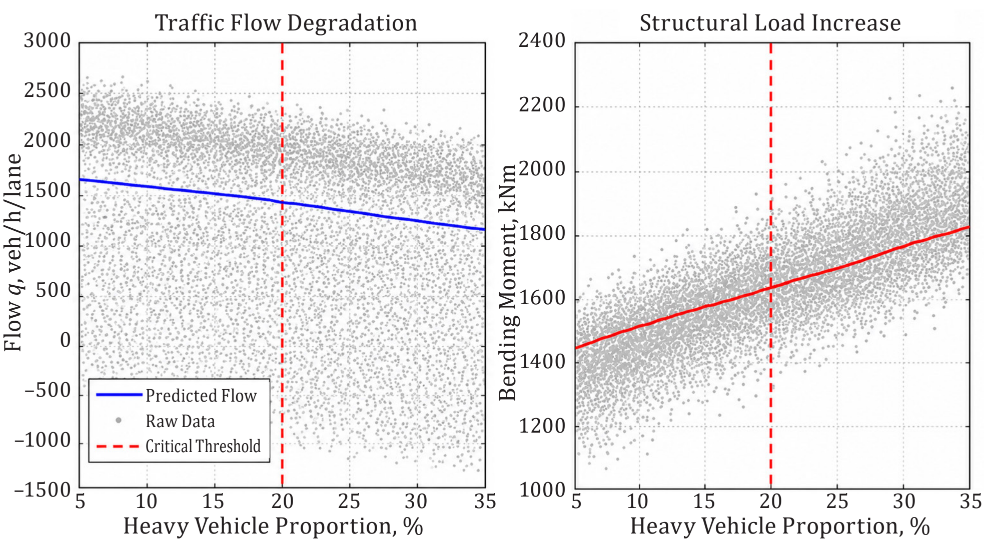

Figure 6. SHAP-based interpretation of the XGBoost structural-response model, showing the interaction effects of heavy-vehicle proportion, traffic density, and inter-vehicle spacing on predicted maximum bending moment

The SHAP interaction surfaces further indicate that these effects are nonlinear. In particular, the combined influence of truck proportion, density, and inter-vehicle spacing becomes more pronounced under peak-hour conditions, when traffic interactions are stronger and multiple heavy-vehicle presence is more likely. The results therefore suggest the existence of a transition region in which further increases in heavy-vehicle share lead to accelerated degradation in both traffic-flow efficiency and structural performance. In the present dataset, this transition became more evident when truck composition approached approximately 20%, beyond which both predicted flow reduction and structural-response amplification increased more rapidly. The predictive performance of the XGBoost models also supports the use of machine learning for estimating the analysed indicators, with strong performance obtained for traffic flow and maximum bending moment prediction. In addition, the correlation analysis reinforced the dominant influence of heavy trucks on the structural-response indicators. However, these findings should be interpreted as feature-attribution results of the trained surrogate models, rather than direct physical measurements of bridge response. Nevertheless, they provide a useful explanatory layer for understanding how heavy-vehicle proportion, traffic density, and spacing jointly influence the WIM-informed traffic and structural indicators analysed in this study.

2.6. Structural load effects

Structural load effects were estimated from the road-WIM-informed axle streams using the influence-line-based procedure described in Section 2. Under the baseline observed traffic condition derived from the cleaned road-WIM dataset, the predicted maximum instantaneous bending moment at midspan reached 1280 kNm, while the predicted maximum instantaneous shear force at the support section was approximately 580 kN. These results indicate that bridge structural demand was sensitive to traffic composition: for each additional 10% increase in heavy-vehicle proportion, the predicted bending moment increased by approximately 8.2%, whereas the predicted shear force increased by approximately 7.5%.

Fatigue-related demand was evaluated using Palmgren-Miner linear damage accumulation. Under the same baseline observed traffic condition, the calculated fatigue damage index was D = 0.15, indicating a moderate level of cumulative fatigue exposure for the bridge under the analysed traffic composition. The corresponding fatigue-damage result is presented in Figure 7. To investigate whether operational measures could reduce structural demand, two non-restrictive mitigation strategies were evaluated: lane management, in which heavy vehicles were organised to reduce unfavourable load distribution and heavy-vehicle interaction effects before bridge entry, and speed harmonization, in which a uniform speed limit of 70 km/h was imposed to improve traffic stability and moderate load-effect variability. The estimated structural effects of these scenarios are summarised in Table 5.

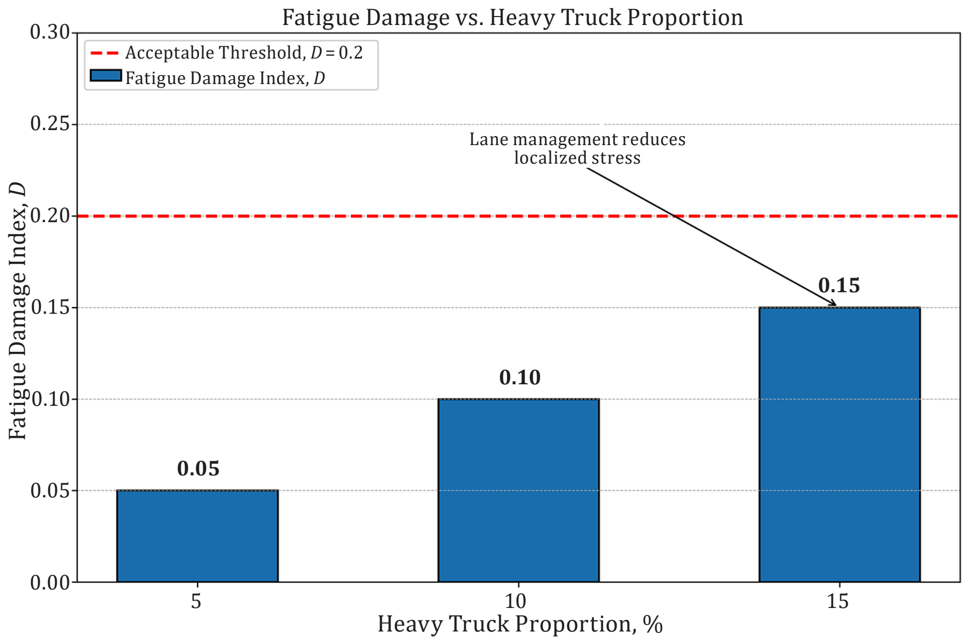

Figure 7. Estimated fatigue damage index under the baseline observed traffic condition, calculated using Palmgren-Miner linear damage accumulation

Compared with the baseline observed traffic condition, both mitigation strategies reduced the predicted maximum bending moment, maximum shear force, and fatigue damage index. In particular, lane management reduced the maximum bending moment from 1280 kNm to 1219 kNm (−4.8%), the maximum shear force from 580 kN to 552 kN (−4.8%), and the fatigue damage index from 0.150 to 0.140 (−6.7%). Similarly, speed harmonization reduced the bending moment to 1235 kNm (−3.5%), the shear force to 562 kN (−3.1%), and the fatigue damage index to 0.144 (−4.0%), as shown in Table 5. These results indicate that even relatively modest operational measures can produce measurable reductions in bridge structural demand and fatigue-related effects. Among the two tested strategies, lane management provided the larger overall reduction in both instantaneous load effects and cumulative fatigue damage, suggesting that traffic-organisation measures targeting heavy-vehicle distribution may offer practical benefits for bridge preservation.

Table 5. Estimated effects of lane management and speed harmonization on maximum bending moment, maximum shear force, and fatigue damage index relative to the baseline observed traffic condition

Intervention	Bending Moment	Shear Force	Fatigue Damage, *D*
Baseline scenario	1280 kNm	580 kN	0.15
Lane Management	1219 kNm (−4.8%)	552 kN (−4.8%)	0.140 (−6.7%)
Speed Harmonization	1235 kNm (−3.5%)	562 kN (−3.1%)	0.144 (−4.0%)

2.7. Simulation-based intervention evaluation

To assess whether operational measures could improve bridge traffic performance while reducing structural demand, two non-restrictive intervention strategies were evaluated using SUMO together with the WIM-informed structural load-effect model described in Section 2. The simulations were performed for the 60 m two-span simply supported bridge carrying two lanes of opposite-direction traffic, with one lane per direction. The simulation inputs were calibrated using the cleaned road-WIM dataset, including traffic demand, vehicle-class composition, speed characteristics, and temporal variation over the daily traffic cycle. The simulated vehicle fleet was represented using the three operational classes defined in Section 3.1, namely C1 (passenger cars), C2 (light trucks), and C3 (heavy trucks), The structural and simulation-based intervention results were evaluated relative to the observed traffic condition derived from the cleaned road-WIM dataset, rather than an assumed heavy-vehicle composition scenario. Therefore, the intervention analysis was based on the observed annual traffic composition and class-specific operating characteristics derived from the cleaned road-WIM data, rather than on simplified example percentages that do not reflect the measured dataset.

Two intervention scenarios were tested. The first was lane management, represented as upstream traffic organisation and truck-lane discipline on the bridge approaches, with the objective of reducing unstable vehicle interactions before entry to the bridge. Because the bridge itself carries only one lane per direction, this measure should be interpreted as a traffic-organisation strategy applied to the approach section and bridge entry conditions rather than as same-direction lane allocation on the bridge deck. The second intervention was speed harmonisation, in which a uniform speed limit of 70 km/h was imposed to reduce speed variability and improve traffic stability. The simulation results are summarized in Table 6. Relative to the baseline scenario, lane management increased flow from 2050 veh/h/lane to 2157 veh/h/lane (+5.2%) and reduced density from 65.0 veh/km/lane to 62.0 veh/km/lane (−4.6%). The associated WIM-informed structural analysis also indicated a reduction in maximum bending moment from 1280 kNm to 1219 kNm

(−4.8%). Similarly, speed harmonization increased flow to 2134 veh/h/lane (+4.1%), reduced density to 64.0 veh/km/lane (−1.5%), and reduced maximum bending moment to 1235 kNm (−3.5%), as shown in Table 6.

Both intervention scenarios produced measurable operational and structural benefits. However, lane management yielded the larger simultaneous improvement in traffic flow and reduction in bending moment, indicating that traffic-organisation measures aimed at moderating heavy-vehicle interactions before bridge entry may be more effective than speed control alone under the analysed traffic conditions. These results are consistent with the broader findings of the study, namely that traffic heterogeneity affects both traffic efficiency and bridge structural demand and that mitigation strategies should therefore be evaluated using both operational and structural criteria.

Table 6. Simulation-based evaluation of intervention scenarios in terms of traffic flow, density, and maximum bending moment

Scenario	Flow, veh/h/lane, SUMO	Density, veh/km/lane, SUMO	Maximum bending moment, kNm
Baseline scenario (observed traffic condition)	2050	65	1280
Lane management	2157 (+5.2%)	62.0 (−4.6%)	1219 (−4.8%)
Speed harmonization (70 km/h)	2134 (+4.1%)	64.0 (−1.5%)	1235 (−3.5%)

3. Discussion

The results of this study show that traffic heterogeneity has a dual influence on bridge operation: it affects both traffic-flow efficiency and bridge structural demand. Using one year of road-WIM data collected on a two-span simply supported bridge in Nanjing, the analysis demonstrated that increasing heavy-vehicle proportion was associated with reduced flow performance, lower average speed, and higher traffic density, while simultaneously increasing the predicted maximum bending moment, maximum shear force, and fatigue-related demand. This confirms that heavy vehicles should not be treated solely as a traffic-flow factor or solely as a structural-loading factor; rather, they are a shared driver of both operational deterioration and increased bridge demand. The calibrated traffic-flow models indicated that higher truck proportions shift the operating state of the bridge section toward less efficient conditions. This finding is consistent with the general understanding that heavy vehicles reduce average speed, increase headway requirements, and lower effective capacity under heterogeneous traffic conditions. In the present study, this effect became more evident as the heavy-vehicle proportion increased, particularly under higher-density conditions. The SHAP analysis further supported this interpretation by identifying heavy-vehicle proportion as the dominant predictor of reduced flow performance. Taken together, these findings suggest that the performance of bridge traffic cannot be adequately interpreted from total demand alone; traffic composition must also be considered.

At the same time, the structural analysis showed that heavier traffic compositions lead to increased bridge demand. The road-WIM-informed moving-load calculations indicated that increasing truck share was associated with larger maximum bending moments and shear forces, as well as higher fatigue-related damage indices. This result is physically reasonable because heavier and more closely spaced axle groups increase both instantaneous load effects and the cumulative number of stress cycles experienced by the bridge. In this sense, the traffic and structural results are mutually reinforcing: the same growth in heavy-vehicle proportion that reduces traffic efficiency also increases structural demand. This coupling is one of the main contributions of the present study. The machine-learning results should be interpreted in this context. XGBoost showed strong predictive performance for traffic flow, maximum bending moment, and maximum shear force, indicating that the processed road-WIM variables contained sufficient information to reproduce these indicators with high accuracy. However, the role of machine learning in this study is not to replace physical bridge analysis or direct bridge monitoring. Instead, it functions as a surrogate predictive layer built on the WIM-informed analytical outputs. The SHAP results are therefore useful because they help explain which variables most strongly influence the model predictions, but they should not be interpreted as direct measurements of bridge behaviour. This distinction is important for avoiding overstatement of the model capability.

A further contribution of the study is the evaluation of mitigation strategies using the integrated framework. Both tested interventions, namely lane management and speed harmonization, produced reductions in structural demand relative to the baseline traffic condition. The results summarised in Table 3 showed that lane management provided the larger overall reduction in maximum bending moment, shear force, and fatigue damage, while speed harmonization also produced measurable but slightly smaller benefits. From an engineering perspective, this suggests that operational strategies influencing the spatial and temporal organisation of heavy vehicles can moderate not only traffic congestion but also structural demand. The benefit is especially relevant for freight-intensive bridge corridors, where agencies must manage mobility and infrastructure preservation at the same time. These findings support the interpretation of the proposed framework as a decision-support methodology. The framework links road-WIM data, traffic-flow analysis, structural load-effect estimation, explainable machine learning, and simulation-based scenario testing in one coherent process. Its value lies in helping practitioners compare candidate management strategies using both traffic and structural indicators. It should therefore be understood as an analytical and scenario-evaluation framework rather than a deployed real-time bridge control system. This clarification is important because the present study demonstrates comparative assessment capability, not autonomous or field-implemented control.

Despite these contributions, several limitations should be acknowledged. First, the analysis is based on data from a single bridge site, and the results may therefore reflect local traffic composition, geometric characteristics, and operational behaviour specific to this corridor. Second, the structural effects were estimated from road-WIM-informed moving-load analysis, not from independently measured bridge strains or displacements. Accordingly, the structural outputs should be interpreted as model-based estimates driven by measured traffic data rather than direct structural-response observations. Third, the vehicle classification scheme and the adopted data-cleaning thresholds may influence the resulting heavy-vehicle percentages and therefore the calibrated relationships. Fourth, the mitigation analysis was conducted through simulation, which necessarily depends on the calibration quality of the SUMO model and the assumptions used to represent driver behaviour, truck acceleration, and lane-changing constraints. There are also limitations associated with the fatigue analysis. The fatigue damage index was derived using Palmgren-Miner linear damage accumulation, which is widely used in engineering assessment but remains a simplified representation of cumulative fatigue processes. The resulting values are therefore most useful for comparative evaluation across scenarios rather than as standalone indicators of remaining service life. Similarly, the machine-learning models were trained and tested on the processed dataset generated within this study; their predictive accuracy should therefore be interpreted as evidence of internal consistency and strong surrogate-model performance, rather than proof of universal transferability to other bridges or traffic environments.

Future work should extend the framework in several directions. Additional bridge sites with different structural systems, span arrangements, and traffic compositions should be examined to test the generalizability of the identified relationships. Greater detail in structural modelling, including site-specific calibration against measured response where available, would further strengthen the interpretation of bending moment, shear, and fatigue results. The mitigation module could also be expanded to include additional operational strategies, such as dynamic truck-routing advice, temporary overtaking restrictions, or adaptive lane control under high freight demand. Finally, the integration of richer contextual variables, such as weather conditions, seasonal variation, and freight scheduling effects, may improve the predictive and explanatory capability of the framework. The present results demonstrate that bridge traffic management benefits from an integrated perspective. Heavy-vehicle heterogeneity degrades traffic performance and increases bridge demand at the same time, and these two effects can be assessed jointly using road-WIM data. By combining traffic-flow modelling, structural load-effect analysis, explainable machine learning, and scenario-based simulation, the proposed framework provides a practical basis for comparing traffic-management measures that aim to balance operational efficiency with infrastructure protection.

Conclusion

This study developed an integrated decision-support framework for evaluating how traffic heterogeneity affects both traffic-flow efficiency and bridge structural demand using road-WIM data collected on a 60 m two-span simply supported prestressed-concrete girder bridge in Nanjing, China. The results showed that increasing heavy-vehicle proportion reduced traffic performance by lowering flow and speed while increasing density, and at the same time increased predicted structural demand in terms of maximum bending moment, maximum shear force, and fatigue-related indicators.

The comparative calibration of the macroscopic traffic-flow models showed that the Underwood's model achieved the lowest RMSE, whereas the Greenshields's model remained a strong and practically useful formulation because of its competitive performance and simpler physical interpretation. The machine-learning results further demonstrated that XGBoost could accurately predict the analysed traffic and structural indicators, while SHAP analysis identified heavy-vehicle proportion as the most influential explanatory factor within the fitted models. The intervention analysis showed that both lane management and speed harmonization improved traffic conditions and reduced structural demand relative to the baseline observed traffic condition, with lane management providing the larger overall reduction in bending moment, shear force, and fatigue-related demand. These findings indicate that bridge traffic management should consider traffic efficiency and structural performance together, rather than treating them as separate problems. The proposed framework should be interpreted as an analytical and scenario-based decision-support methodology, not as a deployed real-time control system. Its main value lies in helping agencies evaluate candidate traffic-management strategies that balance mobility performance with bridge preservation under heterogeneous traffic conditions.

Declarations

Availability of data and materials

The Weigh-in-Motion (WIM) data used in this study were collected from a highway bridge in Nanjing, China, and are subject to data-sharing agreements with the bridge management authority. Due to privacy and security considerations related to infrastructure monitoring, the raw WIM dataset cannot be made publicly available. However, aggregated data and processed results supporting the findings of this study are available from the corresponding author upon reasonable request and with permission from the data provider. The machine learning models, SUMO simulation configurations, and analytical scripts used in this research can be shared to facilitate reproducibility.

Competing interests

The authors declare that they have no competing interests, financial or otherwise, that could have influenced the work reported in this manuscript.

Funding

This research received no specific grant from any funding agency in the public, commercial, or not-for-profit sectors.

Authors' contributions

Jean Claude Sugira: Conceptualization, methodology, data collection and preprocessing, formal analysis, machine learning modeling, traffic simulation, writing – original draft preparation, writing – review and editing, visualization, project administration. Jean de Dieu NINTERETSE: Structural load analysis, fatigue assessment, validation of structural models, writing review and editing. Marc Nshimiyimana: Statistical analysis, data interpretation, writing review and editing. Philemon Niyogakiza: Macroscopic traffic flow modeling, SUMO simulation setup, methodology validation, writing review and editing. All authors have read and approved the final manuscript.

Acknowledgements

The authors would like to express their gratitude to the School of Transportation Engineering and School of Civil Engineering at Southeast University, Nanjing, China, for providing the academic environment and resources necessary to conduct this research. We are deeply thankful to the bridge management authority in Nanjing for granting access to the WIM data that formed the foundation of this study. Special thanks go to our colleagues and peers for their valuable feedback and discussions during the preparation of this manuscript. Finally, we acknowledge the support of our families and friends, whose encouragement and understanding made this work possible.

Statement of the Use of Generative AI and AI-assisted Technologies in the Writing Process

During the preparation of this manuscript, the authors used AI-assisted tools only for language polishing, grammar improvement, and minor formatting support. The research design, data analysis, modelling, interpretation of results, conclusions, and final manuscript content were developed, verified, and approved by the authors. No AI tool was used to generate original research data, fabricate results, or alter the scientific findings. The authors take full responsibility for the content of the manuscript.

REFERENCES

Adresi, M., Abedi, M., Dong, W., & Yekrangnia, M. (2024). A review of different types of weigh-in-motion sensors: State-of-the-art. *Measurement*, *225*, 114042. https://doi.org/10.1016/j.measurement.2023.114042

Blacha, Ł. (2021). Non-Linear Probabilistic Modification of Miner's Rule for Damage Accumulation. *Materials*, *14*(23), 7335. https://doi.org/10.3390/ma14237335

Cartiaux, F.-B., Semiao, J., & Jacob, B. (2023). Performance assessment of a bridge WIM system using optical strands. *Transportation Research Procedia*, *72*, 3940–3947. https://doi.org/10.1016/j.trpro.2023.11.486

Chen, T., & Guestrin, C. (2016). XGBoost: A Scalable Tree Boosting System. *Proceedings of the 22nd ACM SIGKDD International Conference on Knowledge Discovery and Data Mining*, 785–794. https://doi.org/10.1145/2939672.2939785

Claude Sugira, J., Nsengimana, J. P., & Marc, N. (2023). Capacity Analysis Based on Vehicle Trajectory Data on a Weaving Bottleneck in Nanjing. *Engineering Perspective*, *3*(3), 27–34. https://doi.org/10.29228/eng.pers.71385

Dong, Y., Wang, D., Pan, Y., & Ma, Y. (2023). Large field monitoring system of vehicle load on long-span bridge based on the fusion of multiple vision and WIM data. *Automation in Construction*, *154*, 104985. https://doi.org/10.1016/j.autcon.2023.104985

Gokce, H. B., Catbas, F. N., & Frangopol, D. M. (2011). Evaluation of Load Rating and System Reliability of Movable Bridge. *Transportation Research Record: Journal of the Transportation Research Board*, *2251*(1), 114–122. https://doi.org/10.3141/2251-12

González, A., Rowley, C., & OBrien, E. J. (2008). A general solution to the identification of moving vehicle forces on a bridge. *International Journal for Numerical Methods in Engineering*, *75*(3), 335–354. https://doi.org/10.1002/nme.2262

Greenberg, H. (1959). An Analysis of Traffic Flow. *Operations Research*, *7*(1), 79–85. https://doi.org/10.1287/opre.7.1.79

Kockelman, K. M. (n.d.). Modeling traffic's flow-density relation: Accommodation of multiple flow regimes and traveler types. *Transportation*, *28*, 363–374. https://doi.org/10.1023/A:1011815913359

Lopez, P. A., Wiessner, E., Behrisch, M., Bieker-Walz, L., Erdmann, J., Flotterod, Y.-P., Hilbrich, R., Lucken, L., Rummel, J., & Wagner, P. (2018). Microscopic Traffic Simulation using SUMO. *2018 21st International Conference on Intelligent Transportation Systems (ITSC)*, 2575–2582. https://doi.org/10.1109/ITSC.2018.8569938

Lundberg, S., & Lee, S.-I. (2017). *A Unified Approach to Interpreting Model Predictions* (arXiv:1705.07874). arXiv. https://doi.org/10.48550/arXiv.1705.07874

Nowak, A. S., & Szerszen, M. M. (2000). Structural reliability as applied to highway bridges. *Progress in Structural Engineering and Materials*, *2*(2), 218–224. https://doi.org/10.1002/1528-2716(200004/06)2:2%3C218::AID-PSE27%3E3.0.CO;2-8

Roh, C.-G., Park, B.-J., & Kim, J. (2017). Impact of Heavy Vehicles on Highway Traffic Flows: Case Study in the Seoul Metropolitan Area. *Journal of Transportation Engineering, Part A: Systems*, *143*(9), 05017008. https://doi.org/10.1061/JTEPBS.0000077

Ruiz, M., Gualdrón, Ó., Peral Mondaza, J. A., & Mujica Delgado, L. E. (2025). Data Interpretation in Structural Health Monitoring: Toward a Universal Language. *Sensors*, *25*(10), 3054. https://doi.org/10.3390/s25103054

Saifuzzaman, M., & Zheng, Z. (2014). Incorporating human-factors in car-following models: A review of recent developments and research needs. *Transportation Research Part C: Emerging Technologies*, *48*, 379–403. https://doi.org/10.1016/j.trc.2014.09.008

Sugira, J. C., Zhou, X., & De Dieu Ninteretse, J. (2026). An analytical probability distribution model for extreme bridge traffic load effects based on WIM data and extreme value theory. *Advances in Bridge Engineering*, *7*(1), 33. https://doi.org/10.1186/s43251-026-00210-x

Sujon, M., & Dai, F. (2021). Application of weigh-in-motion technologies for pavement and bridge response monitoring: State-of-the-art review. *Automation in Construction*, *130*, 103844. https://doi.org/10.1016/j.autcon.2021.103844

Wang, H., Li, J., Chen, Q.-Y., & Ni, D. (2011). Logistic modeling of the equilibrium speed–density relationship. *Transportation Research Part A: Policy and Practice*, *45*(6), 554–566. https://doi.org/10.1016/j.tra.2011.03.010

Zhao, X., Wang, L., Zhang, Y., Han, X., Deveci, M., & Parmar, M. (2024). A review of convolutional neural networks in computer vision. *Artificial Intelligence Review*, *57*(4), 99. https://doi.org/10.1007/s10462-024-10721-6

Žnidarič, A., & Kalin, J. (2020). Using bridge weigh-in-motion systems to monitor single-span bridge influence lines. *Journal of Civil Structural Health Monitoring*, *10*(5), 743–756. https://doi.org/10.1007/s13349-020-00407-2